THE JOURNAL OF BIOLOGICAL CHEMISTRY VOL. 287, NO. 25, pp. 21346–21355, June 15, 2012

Identification of *NOG* as a Specific Breast Cancer Bone Metastasis-supporting Gene*[S]◆

Received for publication, February 24, 2012, and in revised form, April 30, 2012 Published, JBC Papers in Press, April 30, 2012, DOI 10.1074/jbc.M112.355834

Maria Tarragona[‡1], Milica Pavlovic[‡2], Anna Arnal-Estapé[‡3], Jelena Urosevic[‡4], Mònica Morales[‡], Marc Guiu[‡], Evarist Planet[§], Eva González-Suárez[¶], and Roger R. Gomis[‡‖5]

From the [‡]Oncology Programme and the [§]Biostatistics and Bioinformatics Unit, Institute for Research in Biomedicine (IRB-Barcelona), 08028 Barcelona, the [¶]Cancer Epigenetics and Biology Program (PEBC), Bellvitge Institute for Biomedical Research (IDIBELL), 08908 Barcelona, and the [‖]Institució Catalana de Recerca i Estudis Avançats (ICREA), 08010 Barcelona, Spain

Background: *NOG* gene is required for accumulation of mature osteoclasts and proper skeletal development.
Results: *NOG* mediates breast cancer metastatic bone colonization by osteoclast differentiation and self-renewal metastatic properties.
Conclusion: Expression of *NOG* in breast metastatic cancer cells provides them with bone colonization capabilities.
Significance: The interplay of bone microenvironment and cancer cell autonomous functions define the selection of genes that lead to bone metastasis development.

Metastasis requires numerous biological functions that jointly provide tumor cells from a primary site to seed and colonize a distant organ. Some of these activities are selected for in the primary site, whereas others are acquired at the metastatic niche. We provide molecular evidence showing that the BMP inhibitor, *NOG*, provides metastatic breast cancer cells with the ability to colonize the bone. *NOG* expression is acquired during the late events of metastasis, once cells have departed from the primary site, because it is not enriched in primary tumors with high risk of bone relapse. On the contrary, breast cancer bone metastatic lesions do select for high levels of *NOG* expression when compared with metastasis to the lung, liver, and brain. Pivotal to the bone colonization functions is the contribution of *NOG* to metastatic autonomous and nonautonomous cell functions. Using genetic approaches, we show that when *NOG* is expressed in human breast cancer cells, it facilitates bone colonization by fostering osteoclast differentiation and bone degradation and also contributes to metastatic lesions reinitiation. These findings reveal how aggressive cancer cell autonomous and nonautonomous functions can be mechanistically coupled to greater bone metastatic potential.

Metastasis accounts for most cancer-related deaths (1). Tumor progression is a multistage process in which malignant cells spread from the primary site to colonize distant organs (2, 3). Several genes have been implicated in the various metastasis steps, but very few are mechanistically well characterized (4). A previous screening from our group highlighted the importance of cytokine-cytokine receptor interaction in predicting relapse, which highlights the importance of communication signals within cell types present in the tumor or at the metastasis site (5). Examples of the biological significance of this analysis are TGFβ and bone morphogenic protein (BMP)[6] signaling pathways (5). Perturbations of these signaling pathways are central to tumorigenesis and tumor progression in a cancer cell-dependent and -independent manner (6).

Bone metastasis is a common site of breast cancer metastasis, and bone breakdown is one of the most remarkable clinical features and the major source of morbidity associated with bone metastasis. Breast cancer bone metastases have been predominantly associated with an osteolytic phenotype due to the concerted collaboration between malignant cells and osteoclasts (7). The bone microenvironment is composed of osteoblasts, osteoclasts, mineralized bone matrix, and other cell types embedded within the bone (8). The cross-talk between tumor cells and the microenvironment has been suggested to fuel a "vicious cycle" of tumor growth and bone remodeling (9), which relies on factors secreted by tumor cells that stimulate osteoblast and osteoclast proliferation and maturation, leading to a net increase in osteoclast-mediated bone destruction. Osteoblasts produce and release the receptor activator of nuclear factor-κB (NFκB) ligand (RANKL), which binds to its receptor (RANK) displayed by osteoclast precursors to induce the latter to mature into functional osteoclasts. The osteoblasts may also secret osteoprotegerin (OPG), which acts as a decoy receptor to ambush RANKL, and OPG determines the net rate of bone growth/loss. The BMPs are a family of growth factors that stimulate bone formation by shifting the equilibrium

* This work was supported by the BBVA Foundation, Asociación Española Contra el Cáncer (AECC) Foundation, the Generalitat de Catalunya (Grant 2009 SGR 1429), and the Spanish Ministerio de Ciencia e Innovación (MICINN) (Grant SAF2010-21171) (to R. R. G.).
◆ This article was selected as a Paper of the Week.
[S] This article contains supplemental Figs. 1–5.
[1] Supported by an IRB-Barcelona Ph. D. program.
[2] Supported by a "la Caixa" Ph. D. fellowship.
[3] Supported by a Ph. D. fellowship by the MICINN.
[4] A Juan de la Cierva Researcher (MICINN).
[5] Supported by the Institució Catalana de Recerca i Estudis Avançats (ICREA).
To whom correspondence should be addressed: Oncology Programme, Institute for Research in Biomedicine (IRB-Barcelona). PBB52 Parc Científic de Barcelona, C/Baldiri i Reixac 10-12, 08028 Barcelona, Spain. Tel.: 34-934039959; E-mail: roger.gomis@irbbarcelona.org.

[6] The abbreviations used are: BMP, bone morphogenic protein; RANK, receptor activator of NF-κB; RANKL, receptor activator of NF-κB ligand; OPG, osteoprotegerin; TRAP, tartrate-resistant acid phosphatase; CT, computed tomography; ER, estrogen receptor; KD, knockdown.

between OPG and RANKL to an accumulation of OPG (8). NOGGIN, a BMP antagonist encoded by *NOG*, might shift the equilibrium in the opposite direction, leading to an accumulation of mature osteoclasts (8). BMPs are multifunctional growth factors that belong to the TGFβ superfamily. BMPs were originally isolated by their ability to induce ectopic bone and cartilage formation *in vivo* (10), but also act as multifunctional regulators in morphogenesis during development (10, 11). In bone biology, BMPs have a crucial role in determining the body axis, bone, and cartilage formation in embryonic development, postnatal bone metabolism, and fracture healing (12).

Who produces TGFβ/BMP and how TGFβ/BMP is sensed by stroma and metastatic cells is a matter of great interest. Among the different players that could modulate the TGFβ/BMP signaling pathway and its contribution, we focused on *NOG*, a key player in bone metastasis given its action on bone remodeling processes as well as defining the stroma capacity to maintain cancer stem cells and their niche (13, 14). *NOG* function antagonizes BMPs and is required for neural tissue formation, notochord, and early gastrulation stages (15). *NOG* knock-out shows *NOG* essential function in proper skeletal development (16), suggesting its potential role and contribution in triggering bone remodeling functions, yet its functional role in breast cancer has not been evaluated. Here we report experimental and clinical data indicating that *NOG* is in its own right a powerful double asset for breast cancer metastatic cells to the bone, a provider of stemness and metastatic niche specific capabilities.

EXPERIMENTAL PROCEDURES

Cell Lines—The SKBr3, MCF7, MDA-231, and T47D breast cancer cell lines were obtained from the ATCC. The 1833 and the MCF7 BMd are bone metastatic sublines derived from MDA-231 (17) and MCF7, respectively. These cell lines and their genetically modified variants were maintained in 5% CO_2 at 37 °C in DMEM medium (Invitrogen) supplemented with 10% fetal bovine serum (Biological Industries), 100 units/ml penicillin, 0.1 mg/ml streptomycin, and 0.29 mg/nl glutamine. 293T cells, a lentivirus and retrovirus packaging cell line, were maintained in DMEM supplemented with 10% FBS, 100 units/ml penicillin, 0.1 mg/ml streptomycin, and 0.29 mg/ml glutamine.

Generation of Knockdown and Overexpressing Cells—Stable cell lines expressing the shRNA targeting *NOG* or a nonsilencing shRNA were generated after lentiviral infection. The 293T cells were transfected with packaging vectors and shRNA-carrying vectors (pLKO, from the Sigma-Aldrich Mission shRNA library), and supernatant containing virus was collected 48 h afterward and used for infection of breast cancer cell lines. Infection was done for 24 h in the presence of 8 μg/ml Polybrene. Cells were recovered with fresh medium and selected for 48 h with 4 μg/ml puromycin. The sequence for shRNA NOG is: CCGGGCTAGAGTTCTCCGAGGGCTTCTCGAGAAGCCCTCGGAGAACTCTAGCTTTTTG.

For *NOG* overexpression in SKBr3 cells, *NOG* was cloned into the retroviral vector pBabePuro. As a control, pBabePuro empty vector was used. Retroviral virus was obtained by transfecting 293T cells, and infection was done as described above. After infection, cells were selected with 4 μg/ml puromycin during 48 h. The rescue was done by generating a mutant vector (using the QuikChange multisite-directed mutagenesis kit (Stratagene)) that had synonymous mutation in the *NOG* open reading frame and was insensitive to given shRNA against *NOG*. Hygromycin selection marker was used in the latter case.

Animal Studies and Xenografts—All animal work was approved by the Institutional Animal Care and Use Committee of IRB-Barcelona. BALB/c nude mice of 8–10 weeks of age were used for all studies. For intracardiac injections, 10^5 cells were resuspended in 0.1 ml of PBS and injected into the left cardiac ventricle of the mice, using a 25-gauge needle as described previously (17, 18).

Prior to injection, mice were anesthetized with ketamine (100 mg/kg of body weight) and xylazine (10 mg/kg of body weight), and immediately after injection of tumor cells, mice were imaged for luciferase activity expressed stably by the indicated cell lines using a TK-GFP-luciferase construct described elsewhere (18). Animals were followed once a week using bioluminescence imaging (IVIS Xenogen) to assess bioluminescent activity. For tail vein injection, cells were treated as for intracardiac injection and inoculated in the lateral tail vein. Mice were imaged for luciferase activity immediately after injection and continued to be monitored weekly using IVIS imaging.

Kaplan-Meier Survival and Correlation Analysis—All statistical analysis was performed using Bioconductor. The patient information was downloaded from the Gene Expression Omnibus (GEO) database. Two sets of data were used (a cohort of breast cancer primary tumors GSE12276 and a cohort of metastatic samples from breast cancer patients GSE14020). For each set, *NOG* expression has been standardized to *Z*-score to make measurements comparable. The prognostic effect of *NOG* to predict recurrence-free survival, measured as hazard ratio, was assessed using a multivariate Cox proportional hazards model adjusted by age, hospital of origin, and TNM stage. We measured *NOG* expression-phenotypic (Hazard Ratio of bone recurrence) association using Kaplan-Meier curves.

Quantitative Real-time PCR—Total RNA from subconfluent cells was collected and purified using the PureLink™ mini kit (Ambion) and reverse-transcribed using the high-capacity cDNA reverse transcription kit (Applied Biosystems) following the manufacturer's instructions. Tumorspheres were collected, and RNA was isolated using TRIZOL according to manufacturer's instructions. The final step of elution was done using Qiagen RNeasy mini kit 74104 columns, and reverse transcription was done as described above. Real-time PCR was performed using the TaqMan gene expression assay (Applied Biosystems). Human *NOG*, *ID1*, *ID2*, *RANK*, *RANKL*, *BMP2*, *BMP3*, *BMP6*, *BMP7*, and *B2M* as endogenous control were amplified with the commercially designed TaqMan gene expressions assay and the TaqMan universal PCR master mix (Applied Biosystems). The levels of expression were normalized to endogenous control, and data were analyzed using the comparative $\Delta\Delta C_T$ method. Expression levels of human BMP4 were assessed and normalized to β-actin levels using the SYBR Green real-time PCR reaction (Applied Biosystems) with the following primers:

BMP4F, 5′-GATCCACAGCACTGGTCTTG-3′; BMP4R, 5′-GGGATGCTGCTGAGGTTAAA-3′; β-actin F, 5′-TCACCCACACTGTGCCCATCTACGA-3′; and β-actin R, 5′-CAGCGGAACCGCTCATTGCCAATGG-3′.

In Vitro Proliferation Assay—To assess the proliferation rate between different groups, 5×10^4 cells/well were seeded in p60 tissue culture plates in triplicate. After 4 h, the medium was changed to remove all the nonattached cells, and the concentration at this time point was determined using a cell counter (day 0). Cells were counted at day 1, 3, 5, and 7, and the results were normalized to day 0.

Osteoclast Differentiation Assay—To isolate bone marrow mononuclear cells, 4–6-week-old wild type C57BL/6 mice were sacrificed, their femurs and tibias were flashed with cold PBS solution, and bone marrow mesenchymal cells were cultured in 100-mm dishes overnight in α-minimum Eagle's medium (Invitrogen) medium supplemented with 10% fetal bovine serum, 100 units/ml penicillin, 0.1 mg/ml streptomycin, and 0.29 mg/ml glutamine. After overnight culturing, nonadherent cells were collected and plated in the same medium. After 2 days, the adherent cells were scraped and counted to be plated in 24-well dishes, and osteoclast differentiation was induced by adding the 20 ng/ml RANKL (PeproTech), 30 ng/ml M-CSF (R&D Systems), and conditional medium from breast cancer cells. Medium was changed at day 3, and tartrate-resistant acid phosphatase (TRAP) staining (Sigma-Aldrich) was performed at day 6. Differentiated multinucleated (>3 nuclei) osteoclasts were stained by TRAP staining. Quantification of TRAP-positive ($TRAP^+$) cells was performed, and the average of three independent experiments was plotted with S.D. values.

Tumorsphere Formation Assay—To assess the tumor initiation capability *in vitro*, cells were counted and plated into low attachment 96-well plates at dilution of one cell per well and cultured in tumorsphere media (mammary epithelial basal medium with all supplements and with 20 ng/ml basic FGF and 2% B27 supplement). The process was repeated to ensure second generation tumorspheres. After 2 weeks of culturing, the tumorspheres were counted under the microscope.

Migration and Invasion Assay—Breast cancer cells were seeded in 100-mm tissue culture plates. Upon reaching 100% confluence, a vertical wound was made with a sterile tissue culture tip. Photos of the wound were taken at 0 and 10 h (for 1833 cell lines) and 0 and 20 h (for SkBr3 cell lines) time points. Analysis of wound closure was done by the ImageJ software. For the Transwell invasion assay, 8-μm-pore 24-well plates (Costar) were coated with 0.1% gelatin (Sigma) prior to plating breast cancer cells. shControl, shNOG, and Rescue 1833 cells, as well as control and NOG-expressing SkBr3 cells, were labeled with CellTracker Green and left 24 h in 0.5% FBS cell DMEM medium. Upon that, cells were counted and seeded (60,000 cells/well) in 0.5% FBS DMEM media. Cells were left to migrate on 37 °C for 12 h. Cells were fixed in 10% neutral formalin buffer for 20 min at room temperature. Tumor cells on the top side of the wells were removed with a cotton swab. To quantify cell migration, photos of the bottom side of well were taken, and green cells per field were counted for each condition.

Histopathology and Immunohistochemistry—Hind limb bones were excised, fixed in 10% neutral-buffered formalin, decalcified, embedded in paraffin, and subjected to staining with hematoxylin and eosin (H&E, Richard-Allan Scientific Inc.), anti-Ki-67 antibodies (Novocastra), anti-phospho-Smad 1/5/8 (Cell Signaling), TRAP (Sigma), and anti-caspase-3 (Cell Signaling Tech). Osteoclast number was assessed as multinucleated TRAP-positive cells along the tumor-bone interface on TRAP-stained sections and expressed as the percentage of osteoclast number per perimeter of interface.

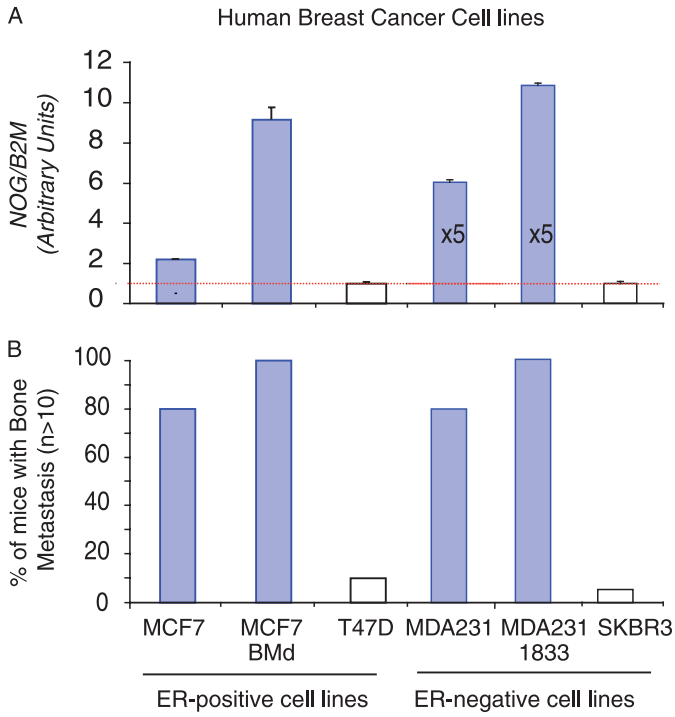

FIGURE 1. ***NOG* expression levels in a panel of breast cancer cells and their experimental bone metastasis ability**. *A*, relative *NOG* expression levels in ER-positive and ER-negative breast cancer cell lines normalized to *B2M* expression levels. Data are mean ± S.D. ($n = 4$). *B*, ability of ER-positive and ER-negative breast cancer cell lines to colonize the bone in an experimental model of metastasis ($n > 10$ mice per cell line). Values were plotted as the percentage of mice developing bone metastasis.

CT Scan Analysis—Development of bone metastasis was monitored by CT imaging (CT-SkyScan). Visible metastatic lesions were measured using the ImageJ software, and the osteolytic area was calculated in mm^2.

RESULTS

Selection of NOG Expression in Bone Metastatic Breast Cancer Cells—We used a panel of well defined breast cancer cell lines (ATCC) originating from patient breast cancer metastasis or primary tumors to evaluate *NOG* expression in breast cancer cells. We correlated the levels of *NOG* expression in those cells with its capacity to form bone metastasis when intracardiacally inoculated in immunocompromised BALB/c nude mice. *NOG* mRNA was detectable in all cell lines. However, the levels varied enormously between them (Fig. 1*A*). Among them, the ER-negative MDA-231 and 1833 cells had the highest level of *NOG* expression (Fig. 1*A*), the 1833 being a bone metastatic cell line derived from the MDA-231 cells (17). A similar increase of *NOG* expression was observed in the ER-positive MCF7 cells that grew in the bones, MCF7 BMd. Cell lines with the higher levels of *NOG* coincide with those with the highest capacity to

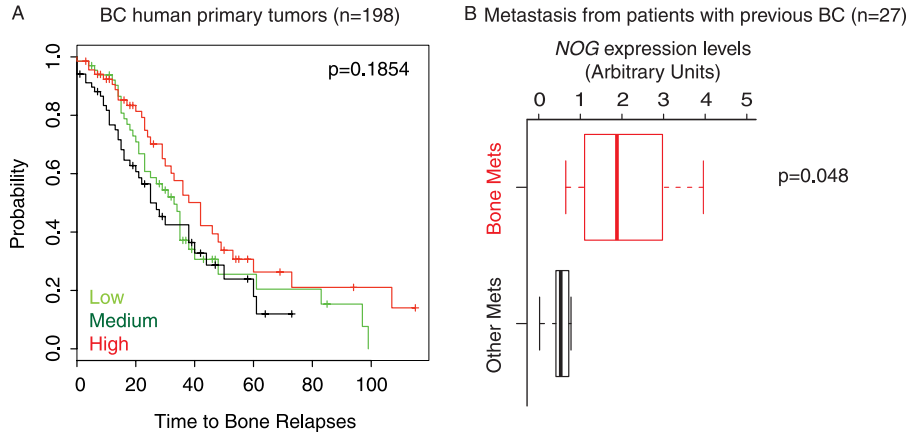

FIGURE 2. ***NOG* expression levels in human primary and metastatic breast cancer samples.** *A*, Kaplan-Meier curves representing the association of recurrence probability with *NOG* expression in human breast cancer (*BC*) cohort (GSE12276). *B*, comparison of *NOG* expression levels at the metastatic (*Mets*) site in a cohort of metastasis, including bone, lung, brain, and liver, from breast cancer patients (GSE14020).

form bone metastasis (Fig. 1*B*). On the contrary, cell lines expressing low levels of *NOG* were not associated with bone metastasis, as is the case with SKBr3 and T47D cells (Fig. 1, *A* and *B*), thus suggesting that *NOG* expression might be necessary but not sufficient because other cell-autonomous requirements have been shown to be necessary to colonize the bone (2). Of note, this association occurred independently of metastasis to soft tissues (supplemental Fig. 1).

NOG Expression Is Associated with Bone Metastasis in Patients—Given the striking association between *NOG* expression and the capacity of breast cancer cells to take and metastasize to the bone, we decided to evaluate to what extent *NOG* levels could predict relapse to the bone in primary breast cancers. Thus, we hypothesized that selection of *NOG* expression in the primary site would endow tumor cells with the ability to efficiently seed the bones, suggesting that *NOG* could be a metastasis progression or initiation gene (4). In breast cancer primary tumors (cohort GSE12276; $n = 198$, including tumors that did relapse to the bone, brain, and lung and tumors that did not relapse), *NOG* mRNA expression levels were not associated with a high probability of relapse to the bone in the patients (Fig. 2*A*), indicating that *NOG* does not predict bone relapse from the primary site. However, when we focus on metastatic samples that originated in patients with a previous episode of breast cancer (GSE14020 (19)), *NOG* levels were up-regulated in bone metastatic lesions as opposed to brain, lung, and liver lesions (Fig. 2*B*). The data reflect a trend of high *NOG* expression in bone metastasis cohort ($n = 27$). Collectively, these results suggest that bone-specific breast cancer metastatic cells select or arise from a population with high *NOG* expression.

NOG Promotes Experimental Bone Metastasis in Vivo—Given the bioinformatics observation of NOG expression in organ-specific metastasis to bone, we thus decided to evaluate the role of *NOG* in a breast cancer bone metastasis experimental model. To this end, we performed experimental bone metastasis assays in nude mice using the 1833 bone metastatic cell line. An 1833 cell line derivative with a knockdown using an shRNA targeting *NOG* (NOG-KD, 70% reduction of NOGGIN protein levels) was used along with cells rescued with a *NOG* mutated form resistant to the shRNA effects and control cells (Fig. 3, *A* and *B*). Changes in the levels of NOG did not result in consistent changes in the BMP-2, -3, -4, -6, or -7 expression levels (supplemental Fig. 2). Following intracardiac injections of tumor cells prelabeled with a luciferase-expressing construct, metastatic progression in the bones was followed via quantitative bioluminescence imaging over the course of 8 weeks. NOG-KD cells had dramatically reduced the probability to form bone metastasis as well as reduced metastatic burden at 1 week after injection, and these differences were maintained throughout the experiment (Fig. 3, *C* and *D*). NOG-KD 1833 cells showed a dramatic reduction (>10-fold) in metastatic burden that was significant ($p < 0.05$, Mann-Whitney *U* test) and was restored upon reintroduction of a mutant *NOG* form resistant to shRNA (Fig. 3*D*). These results highlight that the magnitude of the loss of metastasis phenotype correlated with the efficiency to specifically knockdown *NOG*. To test whether *NOG* expression could affect bone metastasis in a different cell line that expresses low levels of *NOG* and shows a clear inability to colonize the bones, experimental metastasis assays were repeated in SKBr3 cells, which ineffectively colonize the bone although they are very aggressive in *in vitro* models (20). Here again, high levels of *NOG*, a 9-fold increase in NOGGIN protein levels, led to a significant increase in the probability to develop bone metastasis and to a dramatic increase in metastatic burden through the course of the 9-week experiment (>10-fold: $p < 0.05$, Mann-Whitney *U* test) (Fig. 3, *E* and *F*).

To test whether NOG-KD or overexpression affected metastasis elsewhere, control and knockdown 1833 cells and control and overexpressing SKBr3 cells were injected via tail vein of nude mice. We monitored the kinetics of emergence of lung colonization by real-time quantitative bioluminescence imaging of luciferase activity from a stably integrated vector. Neither the control nor the NOG-KD 1833 cells, bone metastatic MDA-231 derivative, were able to colonize the lung 60 days after injection as observed previously for control cells (data not shown) (21). Similarly, neither SKBr3 nor SKBr3-overexpressing *NOG* displayed any capacity to colonize the lungs (Fig. 3*G*).

NOG Functions to Support Breast Cancer Osteolytic Lesions in Bone—As a bone-specific breast cancer metastasis gene, *NOG* could be promoting this phenotype in several possible

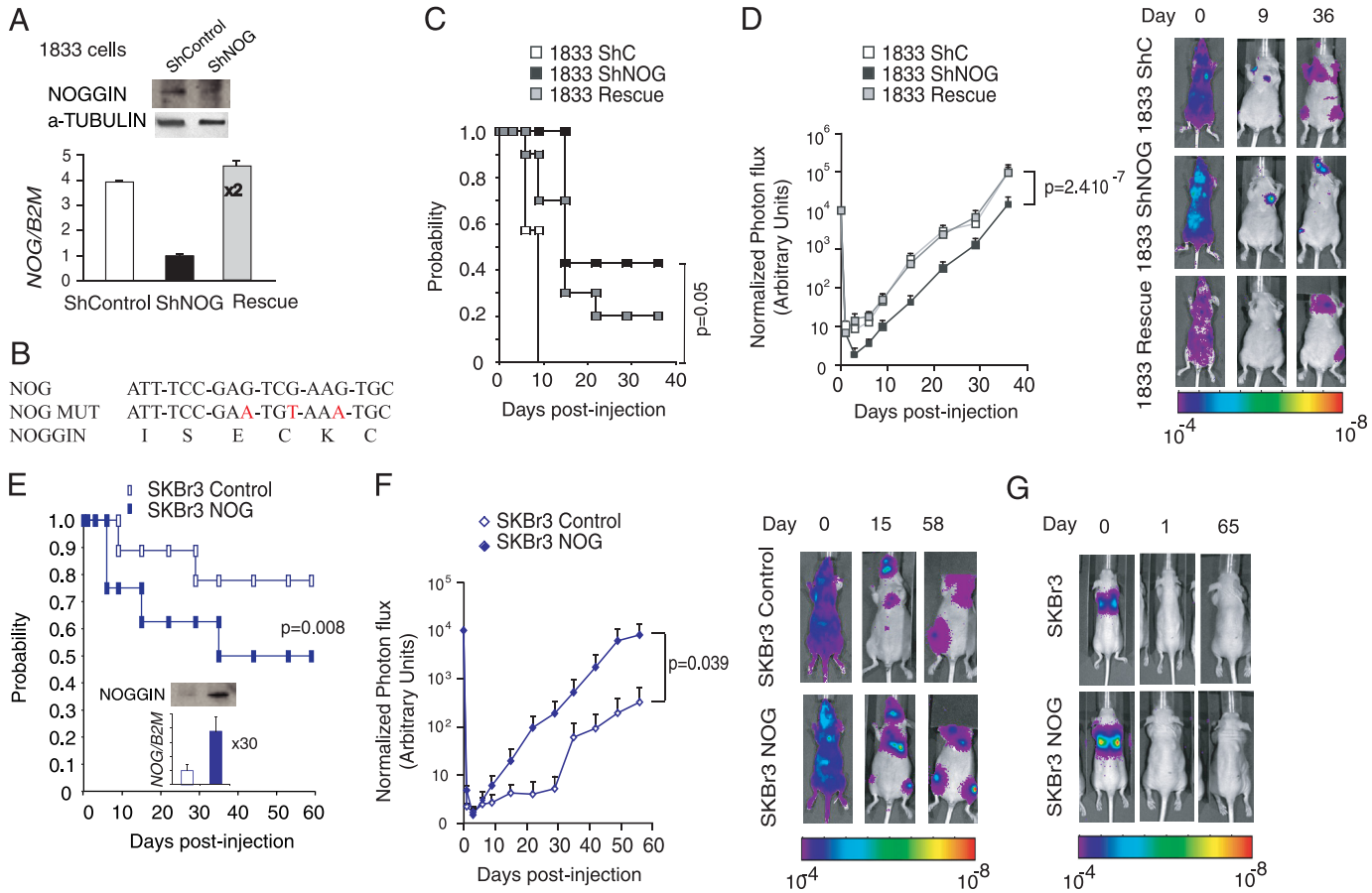

FIGURE 3. ***NOG* mediates experimental bone metastatic abilities of MDA-231-BoM2 1833 and SKBr3 breast cancer cell line.** *A*, *NOG* expression levels in 1833-derived cell lines (shControl, sh*NOG*, and rescue) normalized to *B2M* expression levels. Data are mean ± S.D. ($n = 3$). *Insets* show corresponding protein levels in shControl and sh*NOG* 1833 cells. *B*, a fragment of *NOG* gene sequence targeted by short hairpin RNA with introduced synonymous mutations (*MUT*) indicated in *red*. *C*, Kaplan-Meier bone metastasis-free probability curve of mice inoculated intracardiacally with shControl, sh*NOG*, and Rescue 1833 cells ($n = 10$). *p* value was calculated using the log-rank χ square test. *D*, BioLuminescence imaging curves of bone metastasis development in mice intracardiacally injected with shControl, sh*NOG*, and Rescue 1833 cells ($n = 10$). Representative images are shown. *p* value ($p < 0.05$) was calculated using the Mann-Whitney *U* test. *E*, Kaplan-Meier bone metastasis-free probability curve of mice inoculated intracardiacally with control and *NOG*-expressing SKBr3 cells ($n = 9$). *p* value was calculated using the log-rank χ square test. The *inset* depicts the relative *NOG* expression level normalized to B2M control, as well as corresponding protein levels in SKBr3 control and SKBr3 *NOG* cell lines. Data are mean ± S.D. ($n = 3$). *F*, BioLuminescence imaging curves of bone metastasis development in mice intracardiacally injected with SKBr3 control and SKBr3 *NOG* cell line ($n = 9$). Representative images are shown. *p* value ($p < 0.05$) was calculated using the Mann-Whitney *U* test. *G*, BioLuminescence imaging images of representative mice tail vein injected with SKBr3 control and SKBr3-NOG cells at days 0, 1, and 65 after injection ($n = 7$). Representative images are shown.

ways. We first tested whether *NOG* could affect proliferation by performing *in vitro* assays. No significant differences were observed between control and high or low *NOG*-expressing cells in either assay in 1833 or SKBr3 cells (10^5 cells were plated in *in vitro* experiments (supplemental Fig. 1)). Besides this possible role on proliferation and invasion, we next investigated the role of *NOG* in apoptosis *in vitro* with no results (data not shown). However, to rule out the lack of any phenotype due to the use of an *in vitro* experimental approach, we verified in bone metastatic lesions derived from cells expressing different levels of *NOG* that no significant changes in proliferation (Ki-67 nuclear staining) or apoptosis (cleaved caspase-3 staining) accounted for the differences observed (Fig. 4*A*).

Given that NOGGIN is a BMP inhibitor, and BMP signaling defines the balance between differentiation of bone marrow-derived cells to osteoclast or osteoblasts (8), we investigated the contribution of *NOG* in the formation of osteolytic/osteoblastic lesions. We confirmed in metastatic lesions from 1833 and SKBR3 parental cells that BMP signaling, determined by means of phospho-SMAD1/5/8, was active on bone marrow stromal cells (supplemental Fig. 3). To test whether *NOG* produced endogenously or exogenously by 1833 or SKBr3 metastatic cells could be playing a role in bone remodeling processes, we assessed metastatic burden and bone structure via histomorphometric and CT scan analysis (Fig. 4, *B* and *C*). By histomorphometric analysis, we found that the cells expressing high levels of *NOG*, including control and Rescue 1833 and *NOG*-overexpressing SKBR3 cells, depicted a larger tumor area than their low *NOG*-expressing counterparts, NOG-KD 1833 and control SKBr3 cells, at the same given time after inoculation (Fig. 4, *B* and *C*). Moreover, the CT scan analysis depicted osteolytic metastatic lesions in mice inoculated with breast cancer cells expressing high levels of *NOG* (Fig. 4, *B* and *C*). Differences in the osteolytic area were clearly observed in the experimental setting of the 1833 cells given the highly bone metastatic aggressiveness of these cells. We found that silencing of *NOG* led to a significant 2-fold decrease in osteolytic bone metastatic area when compared with control and Res-

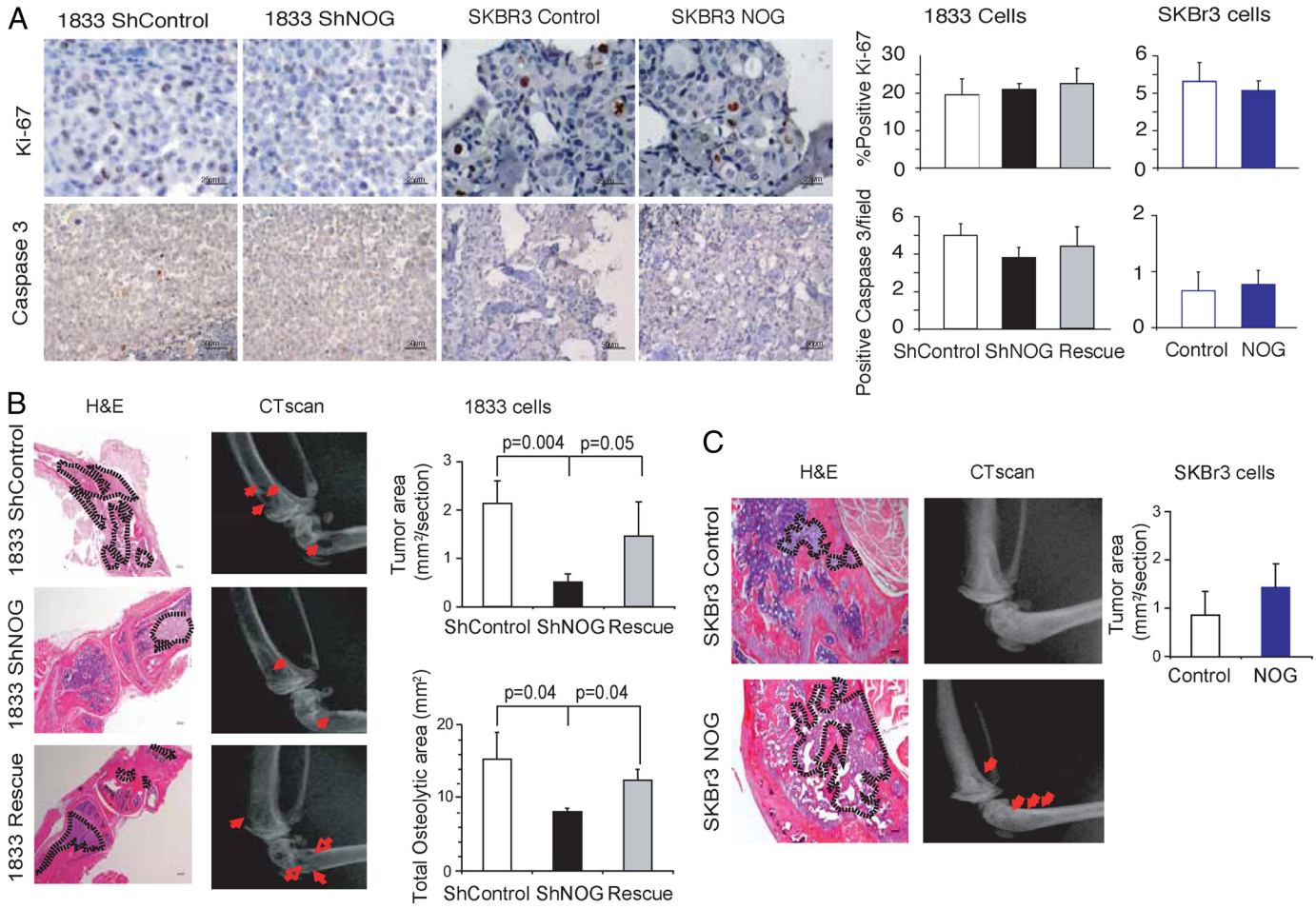

FIGURE 4. **Histological and histomorphometric analysis of 1833 and SKBr3 cells bone metastasis.** *A*, representative bone metastatic lesions from mice intracardiacally injected with shControl, sh*NOG*, and Rescue 1833 and control and *NOG*-expressing SKBr3 cells. Ki-67 (40×) and caspase-3 (20×) staining was performed ($n = 4$). Five different fields per mouse were quantified, and the percentage of positive cells ± S.D. values was plotted. *Scale bar* indicates 25 μm (*upper pictures*) and 50 μm (*lower pictures*). *B* and *C*, representative H&E and x-ray bone metastatic lesions from mice intracardiacally injected with shControl ($n = 10$), sh*NOG* ($n = 5$), and Rescue 1833 ($n = 8$) (*B*) or control ($n = 4$) and *NOG* ($n = 5$)-expressing SKBr3 cells ($n = 3$) (*C*). *Scale bar* = 200 μm. Histomorphometric quantification of the tumor area of bone lesion from each experimental group was performed on H&E stainings and plotted with S.D. values. Quantification of hind-limb osteolysis from mice in each experimental group was done using CT scan analysis and plotted with S.D. values. Representative images are shown; *red arrows* indicate osteolytic bone lesions.

cue 1833 cells (Fig. 4*B*). Quantification of osteolytic bone metastasis area was in agreement with the photon flux results (Fig. 3*D*).

To identify the potential effectors of *NOG*-mediated breast cancer osteolytic bone metastasis phenotypes, we assessed the capacity of breast cancer metastatic cells to trigger osteoclast differentiation at the perimeter of bone metastatic lesions *in vivo*. Osteoclasts are large multinucleated cells found in the bone, whose function is to break down and digest the bone when activated, as opposed to osteoblasts, whose function serves the purpose of bone synthesis. Histological analysis of size-matched tumors showed a decrease in the number of $TRAP^+$ osteoclasts along the bone-metastatic tumor interface, in bone lesions generated by NOG-KD cells, when compared with the controls or Rescue 1833 cells (control and rescue 16.6% ± 3.0, shNOG 9.9% ± 3.0; Fig. 5*A*). To confirm *NOG*-driven osteoclast differentiation in breast cancer bone metastatic lesions, we quantified $TRAP^+$ cells in control and *NOG*-overexpressing size-matched SKBr3 cell bone metastasis, revealing a more than 50% enrichment of osteoclasts/perimeter when lesions are formed by *NOG*-expressing cells (SKBr3 control 14.1% ± 3.1, SKBr3 NOG 22.8% ± 0.4; Fig. 5*A*). To confirm more rigorously the positive stimulation of osteoclast differentiation by metastatic cells *NOG* expression, we performed an *in vitro* osteoclast differentiation assay. The assay consisted of growing primary bone marrow-derived cells from C57BL/6 mice in medium containing a 1:1 ratio of conditioned medium collected from control and NOG-KD 1833 or control and *NOG*-expressing cells and α-minimum Eagle's medium supplemented with macrophage colony-stimulating factor (M-CSF) and RANKL. M-CSF induces the differentiation of murine bone marrow cells into macrophages, and RANKL is an essential cytokine for osteoclastogenesis. Under these conditions, a reduction in phospho-SMAD1/5/8 levels, used as a surrogate of BMP signaling activity, in bone marrow cells was detected when conditioned medium of 1833 *NOG*-expressing cells were used, which was reverted upon NOG-KD or when media not preincubated with 1833 cells were used (Fig. 5*B*). Seven days after initiation of osteoclast differentiation protocol, $TRAP^+$ multinucleated (>3 nuclei) mature osteoclasts were

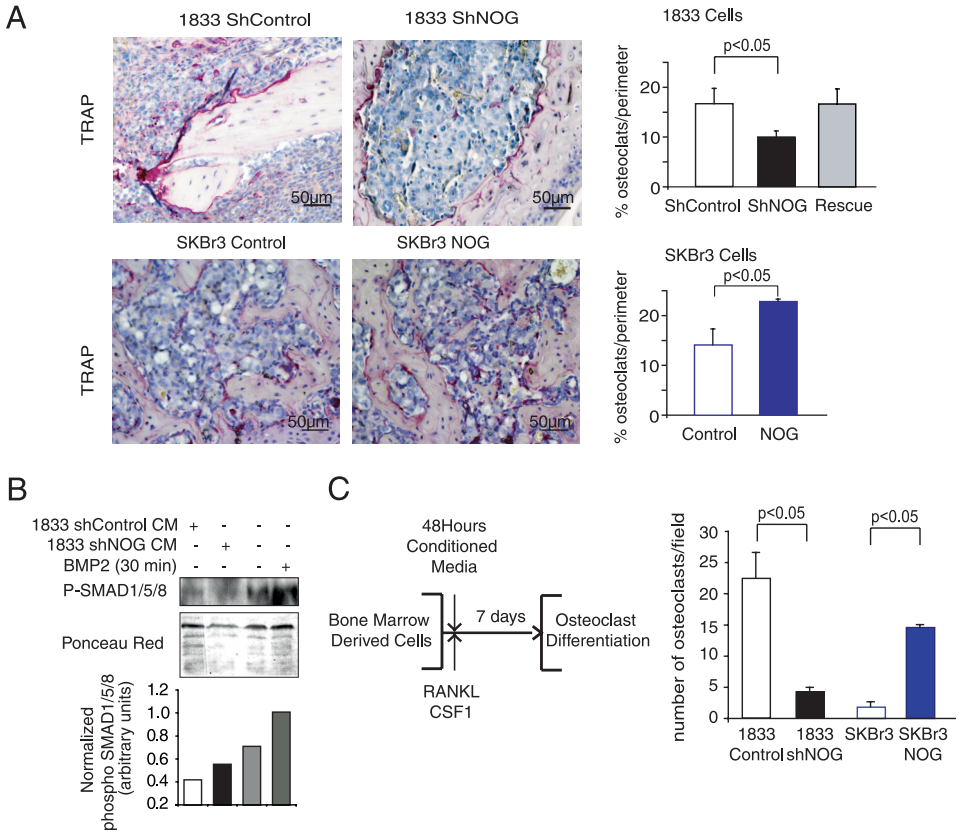

FIGURE 5. ***NOG* enhances metastatic ability of breast cancer cell lines by acting on osteoclast differentiation.** *A*, TRAP staining of representative bone metastatic lesions from mice intracardiacally injected with shControl and shNOG 1833 and control and NOG-expressing SKBr3 cells ($n = 4$). TRAP-positive osteoclast cells (*purple*) along the bone tumor interface were counted in four different fields from four independent mice and plotted with S.D. values. *Scale bar* = 50 μM. *B*, bone marrow cells treated with 50:50 osteoclast differentiation and conditioned medium (*CM*) from 1833 parental and NOG-KD cells or without CM but with human recombinant BMP2 (30 min, 50 ng/ml), were tested for phospho-SMAD1/5/8 (*P-SMAD1/5/8*). Ponceau red staining was used for total protein quantification. *C*, schematic outlines of *in vitro* induction of osteoclast differentiation in murine primary bone marrow cells. Differentiated multinucleated (>3 nuclei) osteoclasts were stained by TRAP staining. Quantification of $TRAP^+$ cells was performed, and the average of three independent experiments was plotted with S.D. values.

scored (Fig. 5*B*). Treatment with conditioned medium derived from cells expressing high levels of *NOG* (1833 and SKBr3-*NOG*) resulted in a 5-fold increase in the number of osteoclasts when compared with NOG-KD 1833 or SKBr3 cells (Fig. 5*C*). No differences in *RANKL* expression were observed in breast cancer cells upon changes in *NOG* expression that could contribute to *in vitro* osteoclast differentiation (supplemental Fig. 4). These results suggest that NOGGIN released by cancer cells is a key player in the metastasis cell-stroma interaction at the bone, which could explain why metastatic cells to the bone but not other tissues select for *NOG* expression.

NOG Expression Contributes to Metastatic Reinitiation at Bone—BMPs have been shown to prevent stem cell renewal of the neural crest and intestinal epithelia stem cells (22). Because NOGGIN is an antagonist of the BMP pathway, *NOG* expression by tumor cells might block its differentiation and enhance the capacity of metastatic cells to migrate, invade, and reinitiate lesions. We corroborated the *NOG* function and BMP signaling on breast cancer metastatic cells, and we performed BMP response element luciferase reporter assays in both SKBr3 and 1833 cells. BMP2 signaling led to a roughly 7–5-fold increase in BMP responsive element (BRE) reporter activity in both cell lines, respectively (supplemental Fig. 3), and overexpression of *NOG* clearly blunted BMP2 activity (supplemental Fig. 3). We did not observe significant and consistent differences in migration or invasion upon changes in *NOG* expression (supplemental Fig. 5). To further validate our hypothesis, we analyzed the ability of the different *NOG*-expressing cell derivatives to form second generation tumorspheres. We observed that the 1833 cells form tumorspheres *per se* in high propensity (Fig. 6*A*), but when *NOG* was down-regulated, this ability was reduced by 80% (Fig. 6*A*). Conversely, when SKBr3 cells underwent the same test, we observed that only 10% of the single cells were able to form tumorspheres, but this was dramatically increased up to 40% upon *NOG* expression (Fig. 6*A*). Interestingly, *NOG* levels also defined the shape of the tumorspheres (Fig. 6*A*). Next, we aimed to address the mechanistic contribution of *NOG* to the reinitiation process. We measured in tumorspheres the expression levels of *ID1* and *ID2*, two well known targets of the BMP pathway that contribute to cell growth, senescence, and negatively regulating differentiation (22), and we also measured the levels of *RANK*, recently described to be key in the expansion of the mammary stem cell compartment in normal breast epithelial cells and in cancer (23, 24) and upstream of *ID2* (25). There was no significant difference in *ID1* levels between groups, whereas the levels of *ID2* and *RANK* changed according to *NOG* levels (Fig. 6, *B* and *C*). Taken together, these data suggest that *NOG* selection in breast cancer metastatic

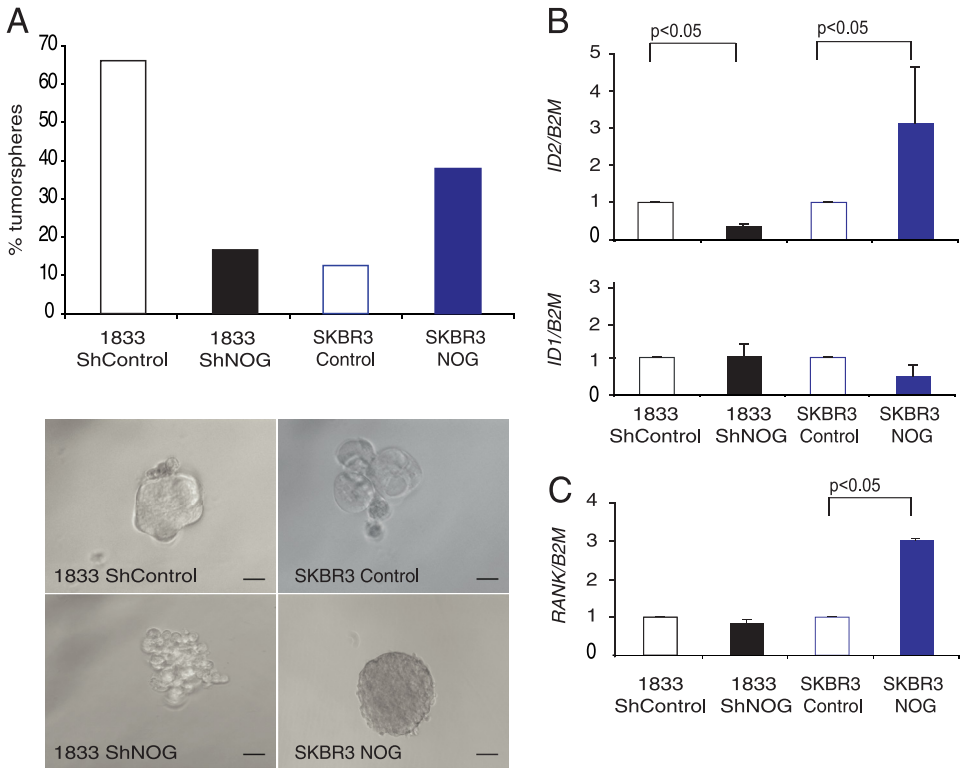

FIGURE 6. ***NOG* enhances tumor initiation ability of 1833 and SKBr3 breast cancer cells.** *A*, shControl and sh*NOG* 1833 cells or control and *NOG*-expressing SKBr3 cells were plated in tumorsphere formation assay *in vitro*. The percentage of tumorspheres formed was calculated, and the average of three independent experiments was plotted. Representative pictures of tumorsphere formed by shControl and sh*NOG* 1833 cells or control and *NOG*-expressing SKBr3 cells were depicted. *Scale bar* = 200 μm. *B*, *ID1*, *ID2*, and *RANK* relative expression levels in control and shControl and sh*NOG* 1833 or *NOG*-expressing SKBr3 cells normalized to *B2M* expression level ($n = 3$).

cells to bone is relevant, providing reinitiation and, particularly, bone metastatic capabilities.

DISCUSSION

NOG has generated high levels of interest in recent years as it has been shown to promote experimental bone metastasis. To date, investigations of how *NOG* promotes such phenotypes have generally focused on osteolytic lesions in the context of prostate cancer (26, 27). However, in comparison, prostate cancer renders osteoblastic lesions (8), whereas osteolytic lesions are largely associated with bone metastasis in breast cancer. Prostate and mammary cancer bone metastases can be osteoblastic or osteolytic, but the mechanisms determining these features are unclear. Bone morphogenetic and Wnt proteins are osteoinductive molecules (28). In prostate, their activity could be modulated by antagonists such as NOGGIN and DICKKOPF-1 (29). The Sonic Hedgehog signaling pathway was shown to augment BMP7 and NOGGIN and to accelerate tumor growth in prostate xenograft (30). This "bone-homing function" was suggested to mediate the interaction between prostate cells and bone stroma. However, the putative contribution of *NOG* in breast cancer has not yet been identified. Here we identified *NOG* to be up-regulated in breast cancer cells with specific capacity to form bone metastasis in experimental models. Our current study provides evidence to link *NOG* expression selection in bone but not lung, brain, or liver metastasis in breast cancer patients irrespective of *NOG* expression in breast cancer primary tumors. The specificity of bone selection for the expression of *NOG* led us to hypothesize that *NOG* provides a key tissue-specific colonization function that makes it unique to bone metastasis.

NOG gene encodes a secreted polypeptide called NOGGIN. NOGGIN is a BMP-specific antagonist protein found to rescue dorsal (head) structures in ventralized *Xenopus* embryo (31). Loss of *NOG* expression has profound effects on development and results in a recessive lethal phenotype at birth (15). *NOG* knock-out mice are characterized by numerous defects: a shortened body axis caudal to the forelimbs with reduced size of somites and neural tube; an open neural tube of varying severity; loss of caudal vertebra; and malformed limbs. Other studies have shown that in the same *NOG* knock-out mouse model, the mouse *NOG* gene is essential for proper skeletal development (16). Examination revealed excess bone and cartilage and failure to initiate joint formation due to excess of BMP activity. Our studies have shown that *NOG*-overexpressing tumor cells acquire a growth advantage in the bone microenvironment, enhancing osteolytic lesions by indirectly activating osteoclast maturation, which is in agreement with the fact that breast cancer cells mostly generate osteolytic bone lesions due to the tendency of breast cancer cells to tip the balance toward enhanced osteoclast activation and trigger bone resorption (7, 32–34). BMP signaling has been shown to be a determinant for the balance between osteoclast/osteoblast differentiation processes by triggering osteoblast differentiation (8). Collectively, we propose an indirect mechanism by which an excess of *NOG*

produced by tumor cells might alter the osteoblast capacity to sense BMP, favoring an excess of osteoclasts and a more osteolytic phenotype of bone metastatic lesions. Moreover, we have shown that *NOG* is a driver of this effect because the activation was observed in the presence of *NOG* and it was lost when *NOG* was depleted. Previous studies have shown that conditioned medium of MDA-231 breast cancer cells induce osteoblast apoptosis *in vitro* (35, 36), which under certain circumstances might add on the *NOG* phenotype described herein.

Not all the cells that get to the metastasis site have the capacity to reinitiate the tumor growth, but only a few of them will be able to reinitiate a lesion (37). These cells have been described as putative breast cancer stem cells. *NOG* as an antagonist of the BMP pathway, a pathway that has been shown to induce the differentiation of cells (38), has been suggested to play a determinant role in preventing the differentiation process elsewhere (22). Moreover, *NOG* has been previously related with the increase of the colon stem epithelial compartment by disabling BMP signaling repression on *de novo* crypt formation (39). Breast cancer stem cells can be isolated by: 1) using nonadherent culture conditions to form tumorspheres and 2) identifying the cells by their surface expression of CD24 and CD44 (37). Our results showed that cells expressing high levels of *NOG* are selected for cancer stem cells because they formed more tumorspheres and resulted in higher numbers of CD24 low CD44 high (data not shown). Indeed, the ability to form tumorspheres was in agreement with the ability of these cells to metastasize into the bone. Moreover, we checked the expression levels of the differentiation regulators *ID1* and *ID2* in the tumorspheres. No significant difference of *ID1* expression was observed among the different groups of tumorspheres. However, *ID2* expression levels were increased in tumorspheres of SKBr3-NOG-overexpressing cells. In agreement with this observation, *ID2* was down-regulated when *NOG* was depleted in the 1833 cells. Moreover, the induction of *ID2* correlated with a higher expression level of *RANK*, which has been described to be key to maintain the pool of mammary stem epithelial cells (24) and is in agreement with previous findings (25). Previous publications have shown that RANKL is responsible for the epithelial cell proliferation in response to progesterone (40) and is the main mediator of the protumorigenic role of progesterone in the mammary gland (23, 41). The luminal cells release RANKL, which binds to the RANK exposed by mammary stem cells (MaSCs) and therefore stimulates the self-renewal process of these cells (42). These results suggested *NOG* as a modulator of breast cancer reinitiation through *ID2* and, subsequently, altering the levels of *RANK* or the other way around. Finally, the expression of high levels of RANK has been linked to resistance to chemotherapy (23), which might open the possibility that metastatic cells expressing high levels of *NOG* are resistant to therapeutic regime in metastatic patients. We interpret the influence of *NOG* into the ability to successfully metastasize, indicating that metastatic cells acquire the ability to home and breach the environment of the bone, but also to endow metastatic cells with metastatic self-renewal activities. Thus, the latter process is likely to take place in a tissue-independent manner as the ability of breast cancer cells to reinitiate a lesion might be independent of the metastatic site. However, if RANK mediated the self-renewal activity, the further requirement for its stimuli, RANKL, driven by the bone environment, might explain why no effect on the primary or other metastatic sites is observed. Collectively, our results suggest that breast cancer bone metastasis cells select for *NOG* expression when metastasizing the bone because its acquisition provides the disseminated cell functions specifically to home, seed, reinitiate, and colonize the bone by enhancing self-renewal functions as well as by altering the bone microenvironment, favoring the activation of osteoclasts.

Acknowledgments—We thank the Functional Genomics and the Advance Digital Microscopy core facilities of IRB-Barcelona.

REFERENCES

1. Sporn, M. B. (1996) The war on cancer. *Lancet* **347,** 1377–1381
2. Gupta, G. P., and Massagué, J. (2006) Cancer metastasis: building a framework. *Cell* **127,** 679–695
3. Sethi, N., and Kang, Y. (2011) Unraveling the complexity of metastasis: molecular understanding and targeted therapies. *Nat. Rev. Cancer* **11,** 735–748
4. Nguyen, D. X., Bos, P. D., and Massagué, J. (2009) Metastasis: from dissemination to organ-specific colonization. *Nat. Rev. Cancer* **9,** 274–284
5. Morales, M., Planet, E., Arnal-Estape, A., Pavlovic, M., Tarragona, M., and Gomis, R. R. (2011) Tumor-stroma interactions a trademark for metastasis. *Breast* **20,** Suppl. 3, S50–S55
6. Massagué, J., and Gomis, R. R. (2006) The logic of TGFβ signaling. *FEBS Lett.* **580,** 2811–2820
7. Mundy, G. R. (2002) Metastasis to bone: causes, consequences, and therapeutic opportunities. *Nat. Rev. Cancer* **2,** 584–593
8. Logothetis, C. J., and Lin, S. H. (2005) Osteoblasts in prostate cancer metastasis to bone. *Nat. Rev. Cancer* **5,** 21–28
9. Guise, T. A., Kozlow, W. M., Heras-Herzig, A., Padalecki, S. S., Yin, J. J., and Chirgwin, J. M. (2005) Molecular mechanisms of breast cancer metastases to bone. *Clin. Breast Cancer* **5,** (suppl.) S46–S53
10. Urist, M. R. (1965) Bone: formation by autoinduction. *Science* **150,** 893–899
11. Wozney, J. M. (1998) The bone morphogenetic protein family: multifunctional cellular regulators in the embryo and adult. *Eur. J. Oral. Sci.* **106,** Suppl. 1, 160–166
12. Canalis, E., Economides, A. N., and Gazzerro, E. (2003) Bone morphogenetic proteins, their antagonists, and the skeleton. *Endocr. Rev.* **24,** 218–235
13. Tang, B., Yoo, N., Vu, M., Mamura, M., Nam, J. S., Ooshima, A., Du, Z., Desprez, P. Y., Anver, M. R., Michalowska, A. M., Shih, J., Parks, W. T., and Wakefield, L. M. (2007) Transforming growth factor-β can suppress tumorigenesis through effects on the putative cancer stem or early progenitor cell and committed progeny in a breast cancer xenograft model. *Cancer Res.* **67,** 8643–8652
14. Mani, S. A., Guo, W., Liao, M. J., Eaton, E. N., Ayyanan, A., Zhou, A. Y., Brooks, M., Reinhard, F., Zhang, C. C., Shipitsin, M., Campbell, L. L., Polyak, K., Brisken, C., Yang, J., and Weinberg, R. A. (2008) The epithelial-mesenchymal transition generates cells with properties of stem cells. *Cell* **133,** 704–715
15. McMahon, J. A., Takada, S., Zimmerman, L. B., Fan, C. M., Harland, R. M., and McMahon, A. P. (1998) Noggin-mediated antagonism of BMP signaling is required for growth and patterning of the neural tube and somite. *Genes Dev.* **12,** 1438–1452
16. Brunet, L. J., McMahon, J. A., McMahon, A. P., and Harland, R. M. (1998) Noggin, cartilage morphogenesis, and joint formation in the mammalian skeleton. *Science* **280,** 1455–1457
17. Kang, Y., Siegel, P. M., Shu, W., Drobnjak, M., Kakonen, S. M., Cordón-Cardo, C., Guise, T. A., and Massagué, J. (2003) A multigenic program mediating breast cancer metastasis to bone. *Cancer Cell* **3,** 537–549
18. Minn, A. J., Gupta, G. P., Siegel, P. M., Bos, P. D., Shu, W., Giri, D. D., Viale,

A., Olshen, A. B., Gerald, W. L., and Massagué, J. (2005) Genes that mediate breast cancer metastasis to lung. *Nature* **436,** 518–524
19. Zhang, X. H., Wang, Q., Gerald, W., Hudis, C. A., Norton, L., Smid, M., Foekens, J. A., and Massagué, J. (2009) Latent bone metastasis in breast cancer tied to Src-dependent survival signals. *Cancer Cell* **16,** 67–78
20. Arnal-Estapé, A., Tarragona, M., Morales, M., Guiu, M., Nadal, C., Massagué, J., and Gomis, R. R. (2010) HER2 silences tumor suppression in breast cancer cells by switching expression of C/EBPβ isoforms. *Cancer Res.* **70,** 9927–9936
21. Padua, D., Zhang, X. H., Wang, Q., Nadal, C., Gerald, W. L., Gomis, R. R., and Massagué, J. (2008) TGFβ primes breast tumors for lung metastasis seeding through angiopoietin-like 4. *Cell* **133,** 66–77
22. Varga, A. C., and Wrana, J. L. (2005) The disparate role of BMP in stem cell biology. *Oncogene* **24,** 5713–5721
23. Schramek, D., Leibbrandt, A., Sigl, V., Kenner, L., Pospisilik, J. A., Lee, H. J., Hanada, R., Joshi, P. A., Aliprantis, A., Glimcher, L., Pasparakis, M., Khokha, R., Ormandy, C. J., Widschwendter, M., Schett, G., and Penninger, J. M. (2010) Osteoclast differentiation factor RANKL controls development of progestin-driven mammary cancer. *Nature* **468,** 98–102
24. Asselin-Labat, M. L., Vaillant, F., Sheridan, J. M., Pal, B., Wu, D., Simpson, E. R., Yasuda, H., Smyth, G. K., Martin, T. J., Lindeman, G. J., and Visvader, J. E. (2010) Control of mammary stem cell function by steroid hormone signaling. *Nature* **465,** 798–802
25. Kim, N. S., Kim, H. J., Koo, B. K., Kwon, M. C., Kim, Y. W., Cho, Y., Yokota, Y., Penninger, J. M., and Kong, Y. Y. (2006) Receptor activator of NF-κB ligand regulates the proliferation of mammary epithelial cells via Id2. *Mol. Cell. Biol.* **26,** 1002–1013
26. Virk, M. S., Alaee, F., Petrigliano, F. A., Sugiyama, O., Chatziioannou, A. F., Stout, D., Dougall, W. C., and Lieberman, J. R. (2011) Combined inhibition of the BMP pathway and the RANK-RANKL axis in a mixed lytic/blastic prostate cancer lesion. *Bone* **48,** 578–587
27. Secondini, C., Wetterwald, A., Schwaninger, R., Thalmann, G. N., and Cecchini, M. G. (2011) The role of the BMP signaling antagonist Noggin in the development of prostate cancer osteolytic bone metastasis. *PLoS One* **6,** e16078
28. Dai, J., Hall, C. L., Escara-Wilke, J., Mizokami, A., Keller, J. M., and Keller, E. T. (2008) Prostate cancer induces bone metastasis through Wnt-induced bone morphogenetic protein-dependent and -independent mechanisms. *Cancer Res.* **68,** 5785–5794
29. Schwaninger, R., Rentsch, C. A., Wetterwald, A., van der Horst, G., van Bezooijen, R. L., van der Pluijm, G., Löwik, C. W., Ackermann, K., Pyerin, W., Hamdy, F. C., Thalmann, G. N., and Cecchini, M. G. (2007) Lack of Noggin expression by cancer cells is a determinant of the osteoblast response in bone metastases. *Am. J. Pathol.* **170,** 160–175
30. Shaw, A., Gipp, J., and Bushman, W. (2010) Exploration of Shh and BMP paracrine signaling in a prostate cancer xenograft. *Differentiation* **79,** 41–47
31. Smith, W. C., and Harland, R. M. (1992) Expression cloning of Noggin, a new dorsalizing factor localized to the Spemann organizer in *Xenopus* embryos. *Cell* **70,** 829–840
32. Steeg, P. S. (2006) Tumor metastasis: mechanistic insights and clinical challenges. *Nat. Med.* **12,** 895–904
33. Taube, T., Elomaa, I., Blomqvist, C., Beneton, M. N., and Kanis, J. A. (1994) Histomorphometric evidence for osteoclast-mediated bone resorption in metastatic breast cancer. *Bone* **15,** 161–166
34. Vukmirovic-Popovic, S., Colterjohn, N., Lhoták, S., Duivenvoorden, W. C., Orr, F. W., and Singh, G. (2002) Morphological, histomorphometric, and microstructural alterations in human bone metastasis from breast carcinoma. *Bone* **31,** 529–535
35. Mastro, A. M., Gay, C. V., Welch, D. R., Donahue, H. J., Jewell, J., Mercer, R., DiGirolamo, D., Chislock, E. M., and Guttridge, K. (2004) Breast cancer cells induce osteoblast apoptosis: a possible contributor to bone degradation. *J. Cell. Biochem.* **91,** 265–276
36. Mercer, R. R., Miyasaka, C., and Mastro, A. M. (2004) Metastatic breast cancer cells suppress osteoblast adhesion and differentiation. *Clin. Exp. Metastasis* **21,** 427–435
37. Clarke, M. F., and Fuller, M. (2006) Stem cells and cancer: two faces of eve. *Cell* **124,** 1111–1115
38. Gazzerro, E., Gangji, V., and Canalis, E. (1998) Bone morphogenetic proteins induce the expression of Noggin, which limits their activity in cultured rat osteoblasts. *J. Clin. Invest.* **102,** 2106–2114
39. Hardwick, J. C., Van Den Brink, G. R., Bleuming, S. A., Ballester, I., Van Den Brande, J. M., Keller, J. J., Offerhaus, G. J., Van Deventer, S. J., and Peppelenbosch, M. P. (2004) Bone morphogenetic protein 2 is expressed by, and acts upon, mature epithelial cells in the colon. *Gastroenterology* **126,** 111–121
40. Beleut, M., Rajaram, R. D., Caikovski, M., Ayyanan, A., Germano, D., Choi, Y., Schneider, P., and Brisken, C. (2010) Two distinct mechanisms underlie progesterone-induced proliferation in the mammary gland. *Proc. Natl. Acad. Sci. U.S.A.* **107,** 2989–2994
41. Gonzalez-Suarez, E., Jacob, A. P., Jones, J., Miller, R., Roudier-Meyer, M. P., Erwert, R., Pinkas, J., Branstetter, D., and Dougall, W. C. (2010) RANK ligand mediates progestin-induced mammary epithelial proliferation and carcinogenesis. *Nature* **468,** 103–107
42. Visvader, J. E., and Smith, G. H. (2011) Murine mammary epithelial stem cells: discovery, function, and current status. *Cold Spring Harb. Perspect. Biol.* **3,** a004879